# Polarization effects during self-focusing with orientation aberration in nematic liquid crystals

A. S. Zolot'ko and V. F. Kitaeva

*P. N. Lebedev Physics Institute, Academy of Sciences of the USSR*
(Submitted 7 February 1986)
Zh. Eksp. Teor. Fiz. **91**, 131–139 (July 1986)

The polarization of rays in a narrow light beam experiencing orientation aberration self-focusing in a homeotropically oriented nematic liquid crystal is studied experimentally and theoretically. Transformation of linearly polarized light into elliptically polarized light and rotation of the plane of polarization (or of the major semiaxis of the polarization ellipse) by up to 90° were observed.

Because of their very pronounced optical anisotropy ($n_e - n_0 \approx 0.1$–$0.2$), nematic liquid crystals can greatly alter the polarization of transmitted light.[1,2] The polarization effects accompanying orientation aberration self-focusing[3,4] of a light beam are of particular interest. In this case, the polarization of the rays transmitted through the nematic liquid crystal (NLC) depends on the spatial distribution of the director field, which becomes nonuniform due to the realignment of the director in the electric field of the narrow beam. This results in self-focusing of the light beam and twisting of the ray trajectories. Moreover, the polarization of the aberration rings and the polarization of the central portion of the aberration pattern both change. The latter effect was discovered in Ref. 3 and is a consequence of the nonplanar distortion of the NLC director field, which is characterized by unequal elastic constants.[5,6] We will not consider it in this paper, which deals instead with the polarization properties of the aberration pattern that accompanies orientation aberration self-focusing of light beams in homeotropic NLCs.

## EXPERIMENTAL RESULTS

Figure 1 shows a sketch of the experimental equipment and configuration. The polarization of the incident light beam from an $Ar^+$ laser ($\lambda = 4880$ Å or $\lambda = 5145$ Å) of power $\leqslant 300$ mW was adjusted by means of a double Fresnel rhombus and was focused by a lens of focal length 280 mm into a cell containing the NLC. Orientation instability developed because the light field distorted the director field of the NLC and thereby altered the local optical properties of the illuminated layer of the crystal, with the result that the light beam was self-focused in the NLC and a characteristic aberration pattern formed in the beam cross section. The aberration pattern was observed by placing a screen $S$ behind the cell in a plane normal to the light beam.

We used a polarizing film to analyze the polarization of the aberration pattern and found that the polarization of the transmitted light differed from that of the incident light. It is helpful to distinguish two types of incidence for the extraordinary light wave on the NLC: 1) oblique incidence at large

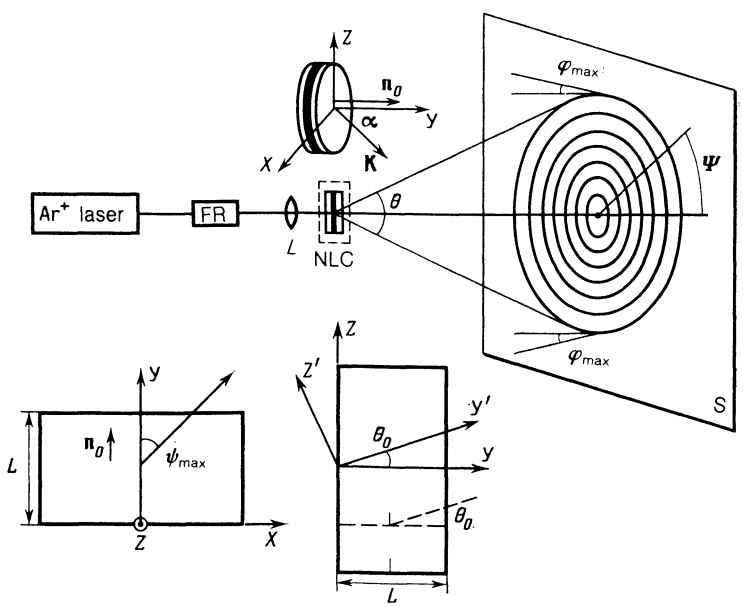


FIG. 1. Experimental system and geometry. The $Ar^+$ laser was a Spectraphysics Model 170 or an ILA-120; FR, Fresnel rhombus; $L$, lens; NLC, nematic liquid crystal; $S$, screen; $\mathbf{k}$, wave vector; $E$, electric field of the light beam; $\mathbf{n}_0$, unperturbed NLC director; $\alpha$, angle between $\mathbf{n}_0$ and $\mathbf{k}_0$; $\theta$, nonlinear divergence angle of the beam outside the crystal ($\theta_0$ is the corresponding value inside the crystal); the angle $\Psi$ is measured in the plane of the screen from the line in which the screen intersects the polarization plane of the light wave; $\psi_{max}$ is the maximum rotation angle of the director in the field of the light wave; $\varphi$ is the rotation angle of the polarization plane (or of the major semiaxis of the polarization ellipse). The octyl-cyano-biphenyl liquid crystal was in the nematic phase for temperatures 32.5 °C $< T_n <$ 40 °C.

 0038-5646/86/070076-05$04.00  

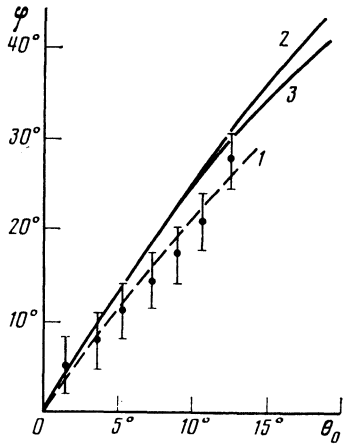


FIG. 2. Rotation angle $\varphi$ of the polarization plane as a function of $\theta_0$, the deflection angle of the ray, for $\Psi = 90°$ and $\alpha = 30°$: 1) experimental dependence; 2) curve calculated in this paper; 3) calculated dependence found using Eq. (13), taken from Ref. 4.

angles $\alpha > 20°$, where $\alpha$ is the angle between the wave vector $k$ of the light wave and the unperturbed director $\mathbf{n}_0$ (Fig. 1); 2) normal incidence, $\alpha = 0$.

For oblique incidence, the rays transmitted by the NLC remain linearly polarized, but the polarization plane is rotated by an angle $\varphi$ that depends on $\alpha$, $\theta$, and $\Psi$ (here $\theta$ is the nonlinear divergence angle for the transmitted beam, and $\Psi$ is the angle measured in the plane of the screen (normal to $\mathbf{k}$) from the line in which this plane intersects the polarization plane of the incident light beam).

For normal incidence, the transmitted rays are elliptically polarized and the rotation angle of the major semiaxis and the ellipticity depend on $\theta$ and $\Psi$. A similar situation occurs when the vertically polarized (ordinary) light wave is normally incident on the crystal.

For a given $\alpha$, the rotation angle $\varphi$ of the polarization plane (or of the semimajor axis of the polarization ellipse) varies at different points in the aberration pattern: $\varphi = 0$ when $\Psi = 0$, and $\varphi = \varphi_{max}$ when $\Psi = 90°$. For constant $\alpha$ and $\Psi$, $\varphi$ increases with $\theta$, i.e., as the distance from the center

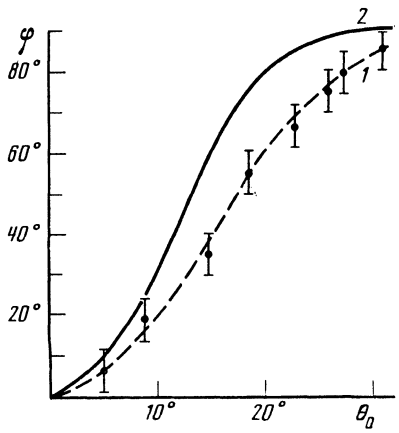


FIG. 3. Rotation angle $\varphi$ of the major semiaxis of the polarization ellipse as a function of $\theta_0$, the ray deflection angle for $\Psi = 90°$ and $\alpha = 0°$: 1) experimental dependence; 2) calculated curve.

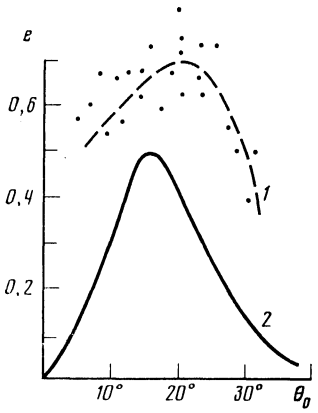


FIG. 4. Ellipticity $e$ vs angle $\theta_0$ for $\Psi = 90°$ and $\alpha = 0°$: 1) experimental curve found by spline approximation[9]; 2) theoretical dependence.

to the aberration ring increases. The rotation angle $\varphi$ has opposite signs in the top and bottom halves of the aberration pattern.

For oblique incidence, $\varphi$ depends on the rotation angle of the analyzer at which the transmitted light is completely extinguished. Measurements using a quarter-wave plate showed that at normal incidence, the transmitted rays were elliptically polarized. We then used a polarizing film (analyzer) to measure $\varphi$ on the outer ring of the aberration pattern as a function of $\theta$, the nonlinear divergence angle of the beam.

Figure 2 shows the experimental dependence $\varphi(\theta_0)$ for $\Psi = 90°$ and $\alpha = 30°$ (curve 1), while Fig. 3 plots $\varphi(\theta_0)$ for $\Psi = 90°$. Here $\theta_0$ is the value of $\theta$ inside the crystal, and Figs. 2 and 3 correspond to oblique and normal incidence, respectively.

We experimentally analyzed the ellipticity $e$ of the transmitted light as a function of the nonlinear refraction angle of the rays forming the external aberration ring for the case when $\alpha = 0$. Here $e$ is defined as the ratio of the lengths of the minor and major semiaxes of the polarization ellipse. The measurements were carried out using a photodiode, which was located in front of the screen and output its signal to a plotter. For each value of $\theta$, the plotter recorded the intensity of the light passing through the film analyzer for various rotation angles of the latter. The ellipticity was cal-

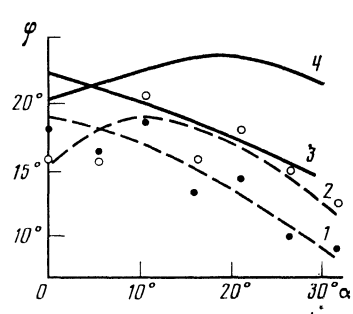


FIG. 5. Rotation angle $\varphi$ of the major semiaxis of the polarization ellipse as a function of the rotation angle $\alpha$ of the crystal for $\theta = 17°$: 1,2) experimental curves for $\Psi = 45°$ and $\Psi = 135°$, respectively; 3,4) theoretical curves.

culated from the ratio of the minimum and maximum intensities:

$$e=(I_{\min}/I_{\max})^{1/2}.$$

Clearly, $e=0$ and $e=1$ correspond to linearly and circularly polarized light, respectively. Curve 1 in Fig. 4 shows the experimental dependence $e(\theta_0)$; we see that $e(\theta_0)$ is nonmonotonic.

We also recorded how $\varphi$ depended on $\alpha$, the rotation angle of the NLC, for a fixed number $N=25$ of aberration rings (this corresponded to a beam divergence $\theta\approx 17°$ outside the crystal) for $\Psi=45°$ and $\Psi=135°$, i.e., in the right and left portions of the aberration pattern. Figure 5 shows the results when the crystal was rotated counterclockwise. We see that the dependence $\varphi(\alpha)$ differs for the right- and left-hand parts of the aberration pattern, and so do the ellipticities—$e$ is greater on the left ($\Psi=135°$) than on the right ($\Psi=45°$). The situation is reversed if the crystal is rotated clockwise, so that the angle $\alpha$ changes sign. We have thus demonstrated experimentally that the polarization of the aberration pattern is not symmetric.

## POLARIZATION OF THE ABERRATION PATTERN: THEORY

To explain the experimental results described above, one must analyze the change in the primary polarization characteristics—the ellipticity $e$ and the rotation angle $\varphi$ of the major semiaxis of the polarization ellipse (or of the polarization plane when $e=0$) from one point to another on the aberration pattern. In other words, we must relate $e$ and $\varphi$ to the angles $\alpha$, $\theta$, and $\Psi$, and the rest of the paper is devoted to this task.

*Starting assumptions and equations.* We assume that an extraordinary light wave ($e$-wave) is incident on a homeotropically oriented NLC of thickness $L$ (the $e$-wave is polarized in the horizontal $xy$ plane, see Fig. 1). The NLC molecules near the wall of the cell are aligned perpendicular to the wall, to which they are rigidly attached. We also assume that: 1) the director is reoriented in the polarization plane of the incident light ($xy$ plane); 2) the angle $\psi$ of rotation of the director from its initial direction (which in general makes an angle $\alpha_0=\arcsin[(\sin\alpha)/\varepsilon^{1/2}]$ with the $y$ axis) depends sinusoidally on the $y$ coordinate; 3) for $y>L/2\cos\alpha_0$, the ray trajectories are straight lines; 4) the polarization of the rays at $y=L/2\cos\alpha_0$ is the same as the polarization of the $e$-wave.

In deriving the equations for the change in polarization of the self-focused light wave transmitted through the NLC, we assume in addition to 1)–4) above that one can neglect the effect of transverse variations in the director field on the rays that produce the aberration pattern. This assumption becomes better justified as the nonlinear refraction angle $\theta$ of the rays decreases.

The unit vector $l$ of a ray emerging from the crystal is specified by the angles $\theta$ and $\Psi$ in the $x, y, z$ coordinate system:

$$l_x=\sin\theta\cos\Psi,\quad l_y=\cos\theta,\quad l_z=\sin\theta\sin\Psi. \tag{1}$$

The vector $l_0$ for a ray leaving the crystal (at the boundary between the crystal and the cell wall) can be expressed in terms of $l$ by the law of refraction:

$$\mathbf{l}_0=\left(1-\frac{1-(\mathbf{n}_0\mathbf{l})^2}{n_{\text{ref}}^2}\right)^{1/2}\mathbf{n}_0-\frac{\mathbf{l}-\mathbf{n}_0(\mathbf{l}\mathbf{n}_0)}{n_{\text{ref}}}. \tag{2}$$

Here $n_{\text{ref}}$ is the refractive index of the NLC, which we set equal to $n_{\text{ref}}=\varepsilon_\perp^{1/2}$.

We consider the Maxwell equations

$$\operatorname{rot}\operatorname{rot}\mathbf{E}=\frac{\omega^2}{c^2}\mathbf{D},\qquad \operatorname{div}\mathbf{D}=0, \tag{3}$$

where

$$D_i=\varepsilon_{ij}E_j,\qquad \varepsilon_{ij}=\varepsilon_\perp\delta_{ij}+\Delta\varepsilon n_i n_j,$$

$\Delta\varepsilon$ is the optical anisotropy, $n_j$ and $E_j$ are the projections of the director and electric field onto the $j$th axis of the cartesian coordinate system, and $\delta_{ij}$ is the Kronecker symbol.

We will solve these equations in an $x'y'z'$ coordinate system with $y'$ axis parallel to the vector $l_0$, $x'$ axis normal to $y'$ and in the horizontal plane, and $z'$ axis normal to the $x'y'$ plane (Fig. 1). In these coordinates the extraordinary and ordinary waves have the slowly varying amplitudes

$$\begin{aligned} A_e&=A_{x'}\cos\beta+A_{z'}\sin\beta,\\ A_0&=-A_{x'}\sin\beta+A_{z'}\cos\beta, \end{aligned} \tag{4}$$

where $\beta$ is the angle between the $x'$ axis and the projection of the director on the $x'z'$ plane; it is equal to

$$\beta=\arccos\left\{\frac{\mathbf{n}-\mathbf{l}_0(\mathbf{n}\mathbf{l}_0)}{[1-(\mathbf{n}\mathbf{l}_0)^2]^{1/2}}\,\frac{[\mathbf{k}'\mathbf{l}_0]}{[1-(\mathbf{l}_0\mathbf{k}')^2]^{1/2}}\right\}, \tag{5}$$

where $\mathbf{k}'$ is the unit vector along the $z'$ axis.

If the light propagates "adiabatically" in the NLC, i.e., if the ordinary and extraordinary waves do not interact,[7] then $\beta$ is equal to $\varphi$, the rotation angle of the polarization plane for the light wave propagating in the NLC (i.e., for the extraordinary wave under the above assumptions).

If the propagation is nonadiabatic, $\beta$ and $\varphi$ are not equal. The angle $\beta$ describes the rotation of the polarization plane for the extraordinary component of the wave, while $\varphi$ is the rotation of the major semiaxis of the polarization ellipse.

Equations (3) imply that the slowly varying amplitudes $A_e$ and $A_0$ satisfy

$$\frac{dA_e}{dy'}=\frac{d\beta}{dy'}A_0+i\frac{\omega}{c}\delta n(y')A_e, \tag{6}$$

$$\frac{dA_0}{dy'}=-\frac{d\beta}{dy'}A_e, \tag{7}$$

where

$$\delta n=\frac{\Delta\varepsilon\varepsilon_\perp}{2\varepsilon_\parallel}(1-(\mathbf{n}\mathbf{l}_0)^2).$$

These equations show that the $o$- and $e$-waves interact because the light wave makes the NLC anisotropic, and the emergent rays are elliptically polarized.

The relations derived in Ref. 8 yield the expression

$$\varphi=\beta+\frac{1}{2}\operatorname{arctg}\frac{A_0A_e^*+A_0^*A_e}{|A_e|^2-|A_0|^2}. \tag{8}$$

for the rotation angle of the major semiaxis of the polarization ellipse. The ellipticity is given by

$$e=\left(\frac{1-\nu}{1+\nu}\right)^{1/2}, \tag{9}$$

where

$$\nu=\left[1+\left(\frac{A_eA_0^*+A_e^*A_0}{|A_e|^2-|A_0|^2}\right)^2\right]^{1/2}\frac{|A_e|^2-|A_0|^2}{|A_e|^2+|A_0|^2}. \tag{10}$$

Relations (6), (7) imply that the *o*- and *e*-waves propagate independently in the NLC when $d\beta/dy'=0$. In this case $\varphi=0$, i.e., rays propagating in the horizontal plane (these are the ones for which $d\beta/dy'=0$ in our geometry) retain the polarization of the incident light.

With the substitutions $\Phi=2(\varphi-\beta)$ and $\Omega=\arccos\nu$, the system (6), (7) simplifies to

$$\begin{aligned}\frac{d\Omega}{dy'}&=\frac{\omega}{c}\delta n\sin\Phi,\\ \frac{d\Phi}{dy'}&=-2\frac{d\beta}{dy'}-\frac{\omega}{c}\delta n\operatorname{tg}\Omega\cos\Phi,\end{aligned} \tag{11}$$

which describes how the polarization changes at any point in the aberration pattern. The Runge-Kutta method was used to solve (11) numerically subject to the supplementary boundary conditions

$$\Omega(0)=0,\quad \Phi(0)=0. \tag{12}$$

*Calculated results.* The calculated polarization characteristics are shown in Figs. 6–8. Figure 6 plots the change in the rotation angle $\varphi$ of the polarization plane for the extraordinary wave (or the rotation of the major semiaxis of the polarization ellipse) and the ellipticity *e* as functions of the *y* coordinate, measured from the center of the crystal to the wall, for nonlinear refraction angles $\theta=5°$ and $\theta=30°$. The *y*-dependence of $\beta$ and the parameter $\mu=\delta n\pi/\lambda(d\beta/dy')^{-1}$ is also shown ($\mu$ is equal to $\pi(d\beta/dy')^{-1}$, the characteristic spatial period over which the polarization of the *e*-wave changes, divided by $\lambda/\delta n$, the spatial beat period for the *e*- and *o*-waves). We see from Fig. 6 that the polarization of the transmitted light does not change significantly ($\varphi$ and *e* are small), and the extraordinary and ordinary waves interact strongly (nonadiabatic propagation) in such a way that almost all the energy contained in the *e*-wave is transferred to the *o*-wave. For $\theta=30°$, the propagation is nearly adiabatic and $\varphi$ and $\beta$ vary in the same way. Figure 6 shows that large changes in the polarization are confined to a narrow layer near the wall. The propagation becomes appreciably nonadiabatic for values $\mu\lesssim 1$, and the increase in the ellipticity *e* is also confined to the wall layer.

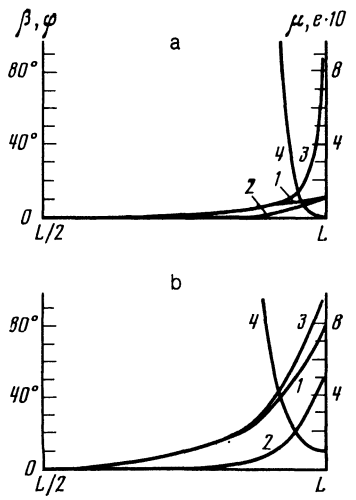


FIG, 6. Polarization characteristics $\varphi$ (curve 1) and *e* (curve 2) and the director field parameters $\beta$ (curve 3) and $\mu$ (curve 4) for aberration self-focusing in the region $L/2<y<L$; $\Psi=90°$, $\alpha=0°$, and $\theta=5°$ (a) and 30° (b).

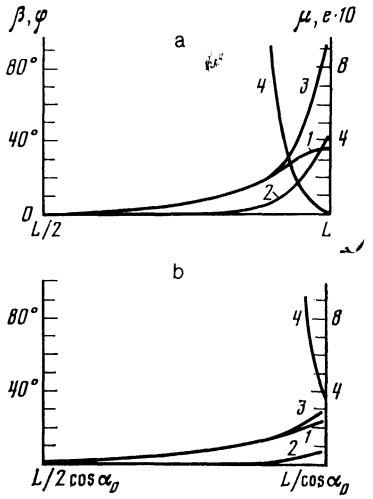


FIG. 7. As in Fig. 6, but for the region $L/2\cos\alpha_0<y<L/\cos\alpha_0$ with $\Psi=90°$, $\theta=17°$, and $\alpha=0°$ (a), 30° (b).

Figure 7 shows how $\varphi$, *e*, $\beta$, and $\mu$ depend on the *y* coordinate for $\Psi=90°$, $\theta=17°$, and two values of $\alpha$. We see that the propagation becomes adiabatic as $\alpha$ increases, because the difference between the refractive indices for the extraordinary and ordinary waves increases and they interact less strongly. It was shown in Ref. 4 that in this case one can use simple formulas from geometric optics to calculate the rotation of the polarization plane; for rays that slant in the vertical plane ($\Psi=90°$), we have the simple result

$$\varphi(\theta)=\operatorname{arctg}(\operatorname{ctg}\alpha\sin\theta). \tag{13}$$

Figure 8 shows how the polarization characteristics change along the *y* axis for the right- and left-hand portions of the aberration pattern. The pronounced asymmetry is due to the asymmetric position of the optically aligned director relative to rays deviating to the left and to the right. An analysis of Figs. 6–8 leads to the following conclusions.

When the spatial period over which the *e*-wave polarization changes is much greater than the effective beat length ($\mu\gg 1$), the light waves propagate adiabatically, $\beta$ is equal to $\varphi$, and the polarization remains linear.

If $\mu\lesssim 1$ then the *e*- and *o*- waves interact, energy is trans-

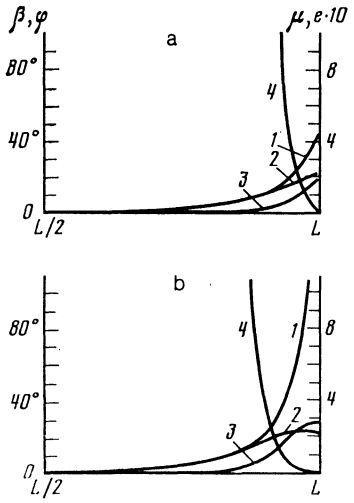


FIG. 8. As in Fig. 6, for the region $L/2 < y < L$ with $\theta = 17°$ and $\alpha = 0°$ for the right ($\Psi = 45°$, a) and left halves ($\Psi = 135°$, b) of the aberration pattern.

ferred from one wave to the other, and the emergent ray is elliptically polarized. Because the wave interaction is confined to a narrow layer near the wall, the above assumption that the rays follow straight-line trajectories is valid.

## COMPARISON OF EXPERIMENTAL AND CALCULATED RESULTS

Figures 2–5 show calculated values in addition to experimental data. We see from Figs. 2 and 3 that the calculated dependence $\varphi(\theta)$ agrees closely with experiment. It should be noted that curve 2 in Fig. 2 was found with allowance for wave interaction but neglects the polarization changes produced by refraction at the outgoing face of the crystal; curve 3 in Fig. 2 ignores possible energy transfer from the *e*-wave to the *o*-wave but treats the refraction exactly.

Equation (13) (curve 3 in Fig. 2) was derived from simple relations in geometric optics; it also closely approximates the experimental data.

The calculated $\theta$-dependence of the ellipticity $e$ (Fig. 4) has the same qualitative form as the experimental curve. The quantitative discrepancy may be ascribed partly to the crudeness of the theoretical model and partly to the presence of background radiation due to scattering by inhomogeneities in the crystal, for which no exact treatment seems possible.

We note that our analysis has assumed that the director is rigidly immobilized at the walls of the cell. If the director could rotate here, this would naturally influence the polarization of the light (some estimates are given in Ref. 10). According to Fig. 5, the calculated curves $\varphi(y)$ for the right ($\Psi = 45°$) and left halves ($\Psi = 135°$) of the aberration pattern also correctly reproduce the experimental results.

In summary, we have shown that when orientation aberration self-focusing of a narrow light beam occurs in nematic liquid crystals, the polarization of the transmitted light differs greatly from the incident polarization—linearly polarized normally incident light becomes elliptically polarized, while obliquely incident light remains linearly polarized, but both the position of the polarization plane and the position of the major semiaxis of the polarization ellipse vary asymmetrically over the beam cross section in a way that depends on the beam divergence angle.

The experimental results are fully explained by a simple physical model for the interaction of a narrow light beam with a nematic liquid crystal which allows for the spatial distribution of the director field in the beam and for the twisting of the rays during self-focusing.

In closing we would like to thank N. N. Sobolev for his interest in this work and for helpful discussions, M. P. Ermilova for assistance, and Yu. E. Voskoboĭnikov for doing the spline calculations.

[1]L. M. Blinov, Élektro- i Magnitooptika Zhidkikh Kristallov (Electro- and Magnetooptics of Liquid Crystals), Nauka, Moscow (1978).
[2]V. V. Zheleznikov, V. V. Kocharovskiĭ, and Vl. V. Kocharovskiĭ, Usp. Fiz. Nauk **141**, 257 (1983) [Sov. Phys. Usp. **26**, 877 (1984)].
[3]A. S. Zolot'ko, V. F. Kitaeva, N. N. Sobolev, and L. Chillag, Pis'ma Zh. Eksp. Teor. Fiz. **32**, 170 (1980) [JETP Lett. **32**, 158 (1980)].
[4]A. S. Zolot'ko, V. F. Kitaeva, N. N. Sobolev, *et al.*, Zh. Eksp. Teor. Fiz. **83**, 1368 (1982) [Sov. Phys. JETP **56**, 786 (1982)].
[5]B. Ya. Zel'dovich and N. V. Tabiryan, Zh. Eksp. Teor. Fiz. **82**, 1126 (1982) [Sov. Phys. JETP **82**, 656 (1982)].
[6]S. M. Arakelyan and Yu. S. Chilingaryan, Nelineĭnaya Optika Zhidkikh Kristallov (Nonlinear Optics of Liquid Crystals), Nauka, Moscow (1984), Chap. 5.
[7]N. Kroo, L. Chillag, I. Yanoshi, *et al.*, Izv. Akad. Nauk SSSR Ser. Fiz. **47**, 2027 (1983).
[8]M. Born and E. Wolf, *Principles of Optics*, 6th ed., Pergamon (1980).
[9]Yu. E. Voskoboĭnikov, N. G. Preobrazhenskiĭ, and A. I. Sedel'nikov, Matematicheskaya Obrabotka Éksperimenta v Molekulyarnoĭ Gazodinamike (Mathematical Analysis of Experimental Data in Molecular Gasdynamics), Nauka, Moscow (1984).
[10]A. S. Zolot'ko, V. F. Kitaeva, and N. N. Sobolev, FIAN Preprint No. 100, Moscow (1984).

Translated by A. Mason